2F

PNL-2954
UC-70

Tests for Determining Impact Resistance and Strength of Glass Used for Nuclear Waste Disposal

L. R. Bunnell

May 1979

Prepared for the U.S. Department of Energy
under Contract EY-76-C-06-1830

Pacific Northwest Laboratory
Operated for the U.S. Department of Energy
by Battelle Memorial Institute

Battelle

PNL-2954

NOTICE

PACIFIC NORTHWEST LABORATORY
operated by
BATTELLE
for the
UNITED STATES DEPARTMENT OF ENERGY
Under Contract EY-76-C-06-1830

Printed in the United States of America
Available from
National Technical Information Service
United States Department of Commerce
5285 Port Royal Road
Springfield, Virginia 22151

Price: Printed Copy $____*; Microfiche $3.00

*Pages	NTIS Selling Price
001-025	$4.00
026-050	$4.50
051-075	$5.25
076-100	$6.00
101-125	$6.50
126-150	$7.25
151-175	$8.00
176-200	$9.00
201-225	$9.25
226-250	$9.50
251-275	$10.75
276-300	$11.00

PNL-2954
UC-70

TESTS FOR DETERMINING IMPACT RESISTANCE AND STRENGTH OF GLASS USED FOR NUCLEAR WASTE DISPOSAL

L. R. BUNNELL

MAY, 1979

Prepared for the
U. S. Department of Energy
under contract EY-76-C-06-1830

Pacific Northwest Laboratory
Richland, Washington 99352

SUMMARY

Tests are described for determining the impact resistance (Section A) and static tensile strength (Section B) of glasses containing simulated or actual nuclear wastes. This report describes the development and use of these tests to rank different glasses, to assess effects of devitrification, and to examine the effect of impact energy on resulting surface area. For clarity this report is divided into two sections, Impact Resistance and Tensile Strength.

TABLE OF CONTENTS

LIST OF FIGURES

A. IMPACT RESISTANCE

A.1 INTRODUCTION

Among the various means of disposing of high-level radioactive wastes, a leading candidate at present is to incorporate them into a glass and place this glass in a metal canister of quite large size, of the order 0.6 m in diameter and 3 m long. As a consequence of accidents during handling and shipping it is possible that an occasional canister could undergo impact. If an unprotected canister interacts with a hard unyielding surface, its mass assures that the glass will be severely damaged in the impact area. The loss of respirable or dispersible fine particles then depends on (1) whether such fines are generated by impact, (2) the integrity of the canister, i.e., whether it is breached by the impact, and (3) the external environment, such as moving air or water.

Only the first of these is addressed here, since it is a property of the waste form itself. The second and third are so dependent on canister design and local conditions as to be more readily addressed by other disciplines.

The purpose of this work was to develop and assess a laboratory method for evaluating the impact resistance of simulated and actual waste-containing glasses. As a laboratory test, it is recognized that the approach would be limited to comparing different glass types and to perhaps be useful in comparing glass to other candidate waste forms. It is not intended that this work would replace large-scale drop tests using actual large canisters filled with simulated waste glasses. Those tests have been done in the past[1] and cannot be completely replaced by the more idealized laboratory test. The lab-scale impact test should at least decrease the number of large-scale tests which are done because it should provide a means to judge whether small composition or processing changes are likely to have a major effect on impact characteristics.

A.2 EXPERIMENTAL METHOD

The general approach taken in this work is similar to that used by other groups in the field of radioactive waste disposal.[2,3] A glass specimen,

usually in the form of a right circular cylinder, is placed in a cavity between a hardened steel punch and die, and a known weight falling through a known distance is used to impact the glass. A drawing of the impact machine is shown in Figure 1, and Figure 2 shows the die. The cavity in the die is left purposely large to preclude any constraint or support provided by the die. Thus, the specimen is assumed to absorb most of the impact energy and is converted to a compact of powder in the bottom of the die. Except when otherwise noted, the specimen was always 1.2 cm long and 1.1 cm diameter, and was impacted as shown in Figure 2.

The large die size relative to the specimen diameter resulted in a quantity of air being expelled from the die during impact; this tended to pump fine particles, amounting to >1% of the sample mass. An aluminum foil hood was useful in decreasing losses, but retrieval of particles from the wrinkled foil was difficult. The final solution was to machine swirl chambers into the punch to provide a zone of lower air velocity. These chambers decreased sample loss to <0.4%, which was regarded as acceptable.

The prime method for evaluating the size of particles >37 μm was by sieving. The type of sifter used* was well adapted to small sample quantities and fine particles. The glass shards were shaped such that screen blinding was a significant problem; glass could not be quantitatively removed for weighing except ultrasonically, so screens were weighed each time before sieving and then subtracted from the weight of screen plus glass. The sieving results were then plotted as percent finer than a given size and appear extensively in this report. The scatter among results on a given glass type was ±5%.

Sieving was quite ineffective for the particles below 325 mesh (44 μm) which are of the most interest for dispersibility. When screens to 5 μm were tried, agglomeration was a severe problem; a sedimentation technique† was used. In this method, the particles were allowed to settle in a column of a suitable liquid, and the attenuation of an x-ray beam passing through the liquid and suspended particles was measured. By means of Stokes' Law, an

---

*Sonic Sifter, ATM Corp., Milwaukee, WI.

†Sedigraph 5000, Micromeretics Corp., Norcross, GA.

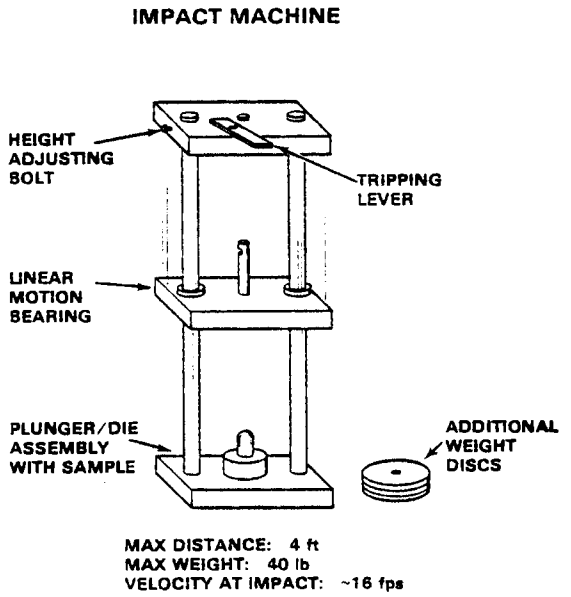

Figure 1. Drawing of the impact machine. The weight is constrained on linear bearings

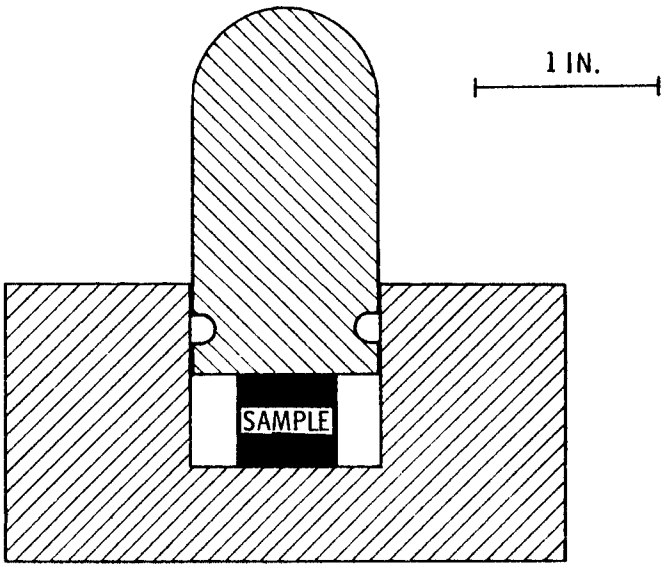

Figure 2. Sectional view of the punch and die arrangment. The insets shown in the punch are swirl chambers.

equivalent spherical diameter was calculated. The device works well in the less than 100 μm range and can detect particles to a size limit determined by the density and the settling time allowed by the experimenter. This method was used to assess the dispersible fraction (<10 μm) produced in our tests. It is estimated to be accurate to ±15% and reproducible to ±5%.

The surface area created by impact is a critical parameter in leaching performance, so this quantity was determined by using the standard B.E.T. (Brunauer, Emmett and Teller) method. We were particularly interested in the relationship between surface area and the impact energy, so this property was measured over a wide range of impact energies for several glasses.

A.3 EXPERIMENTAL RESULTS AND DISCUSSION

A.3.1 Ranking of Glasses as a Function of Impact Energy.

Three model glasses, fused silica, soda-lime-silica plate glass, and 73-1* frit, were used to examine the effects of varying impact energy over an order of magnitude. Figure 3 shows the results. It is seen that the ranking of these three glasses is not changed over this range of energies, and fused silica is always the worst performer (greatest fine particle production), while 73-1 frit is always best. Since impact energies during handling/transportation accidents are expected to be 10^5-10^6 J, the 217J (160 ft-lb) limit of the machine was used extensively as a standard impact energy. At the 217J limit, the weight was moving its fastest at 4.88 m/sec (16 ft/sec) and is thus closest to a relevant impact velocity.

A.3.2 Multiple Impact Damage.

It has been reported[2] that multiple low-energy impacts can be used to approximate high-energy single impacts. In view of the large geometrical difference between the solid right circular cylinder of the first impact and the bed of powder of the subsequent impacts, this contention appeared suspect.

---

*For convenience, glass compositions have been referred to by number designations having only local meaning. The Appendix contains a table of chemical compositions. Table 1 gives a brief description of the glasses.

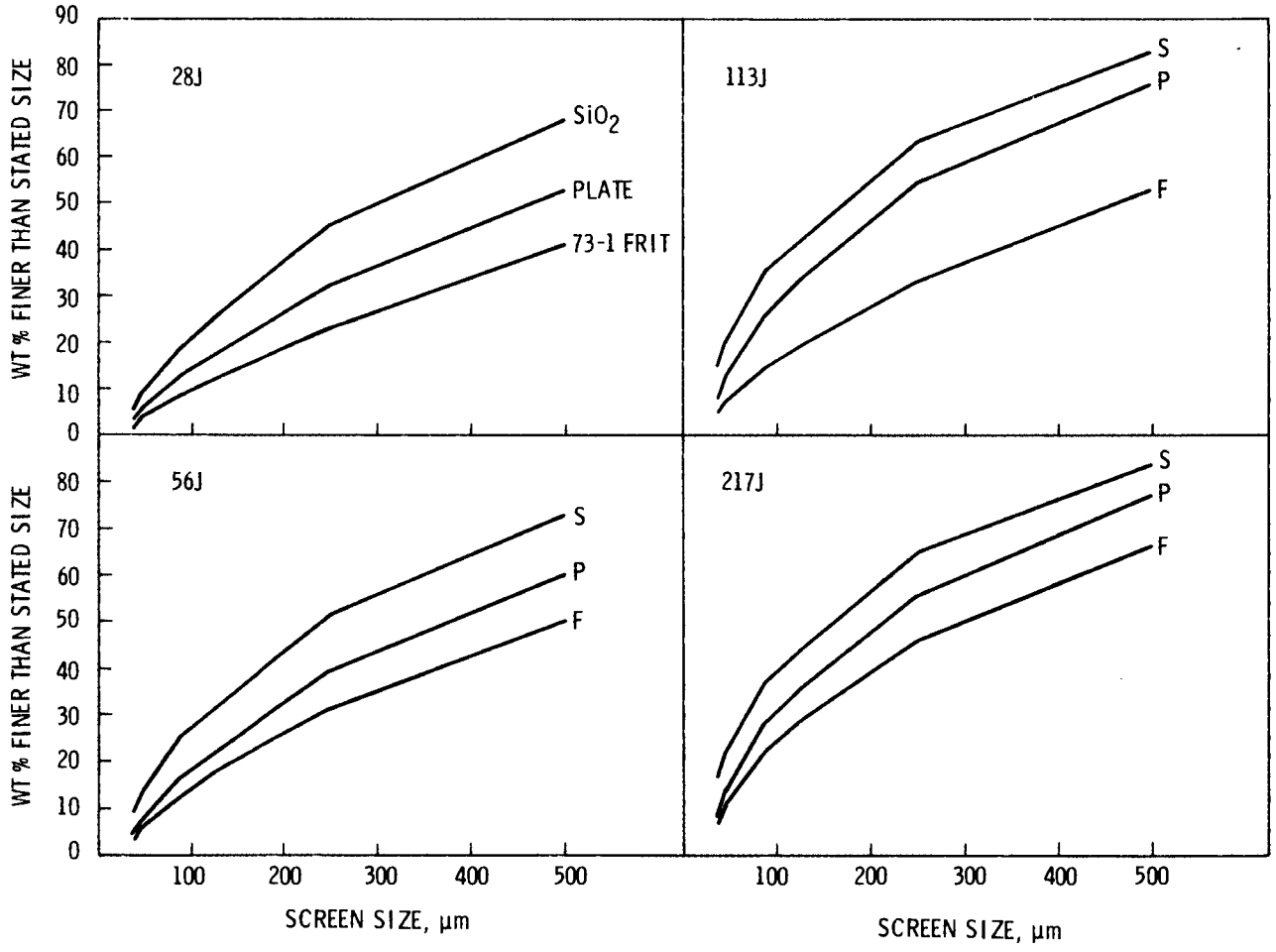

Figure 3. Sieve analysis results for three glasses, over a range of impact energies. Lines are drawn through data averaged over three impacts; scatter was typically ±5%.

TABLE 1. Brief Description of Glasses Which Were Impact Tested

Designation	Description
72-68 (Vitreous)	Nonradioactive candidate waste glass made with 73-1 frit and one of the Pw-4b calcines.
Fused SiO_2	Commercially available fused silica obtained as transparent sheet.
77-GM-09	Natural volcanic glass, Glass Mountain, Siskiyou County, CA., 500 yr. old.
72-G-004	Natural volcanic glass, Long Valley Caldera, Moro County, CA., 70,000 yr. old.
77-OM-01	Natural volcanic glass, Obsidian Mound, Moro County, CA., 5000 yr. old.
76-68	Nonradioactive candidate waste glass made with 76-101 frit and PW-8a-3 calcine.
77-260 (Vitreous)	Nonradioactive version of the AGNS glass composition.
Soda-Lime-Silica	Commercially available window (plate) glass.
ICM-11	The glass used in In-Can-Melter Test #11. Composition was PW-7-2 calcine and 73-1 frit, 1:2.
73-1	The frit used to produce 72-68 glass.
76-101	The frit used to produce 76-68 glass.

As a test, the same amount of energy, 217J (160 ft-lb) was delivered to a sample of soda-lime-silica glass as 1, 2, 3, 4 or 8 impacts, varying the weight/height combination to produce equal damage energies. The bed of particles was stirred after each impact to increase the potential for damage. The velocity of the hammer varied, of course, with height, but not by more than a factor of two (4.88 m/sec versus 2.44 m/sec). Figure 4 shows the size fractions produced in this test; the results are certainly not equivalent and show the expected particle grinding effect. After two impacts, the results are closely grouped, reflecting the decreasing efficiency of generating particles. Multiple low-energy impacts do not appear to be a workable means to approximate high energy single impact events.

A.3.3 Specimen L/D Ratio

In a single-blow impact test, the length/diameter ratio (L/D) of the specimen could influence the results. Since the test method might be applied to different geometries, it was considered important to know how specimen geometry affected the results. A rod of soda-lime-silica glass, 1.3 cm diameter, was obtained and cut into different lengths, from 0.64 to 6.4 cm. These were impacted in a special long die at a constant energy of 193J (142 ft-lb). The results are plotted in Figure 5. It is seen that the L/D has a fairly large influence on the results; an order-of-magnitude change in L/D ratio changed the weight percent finer than 100 μm by a factor of about 3.

Surface areas of the powders can be calculated based on sieve analysis and the assumption of perfect spheres. As shown in the insert in Figure 5, the efficiency of surface area production drops as sample length increases. For the purposes of all testing reported here, the sample length was held at 1.2 cm x 1.1 cm diameter. If that was impossible, soda-lime-silica glass identical to the specimen was used to help establish a link to existing results.

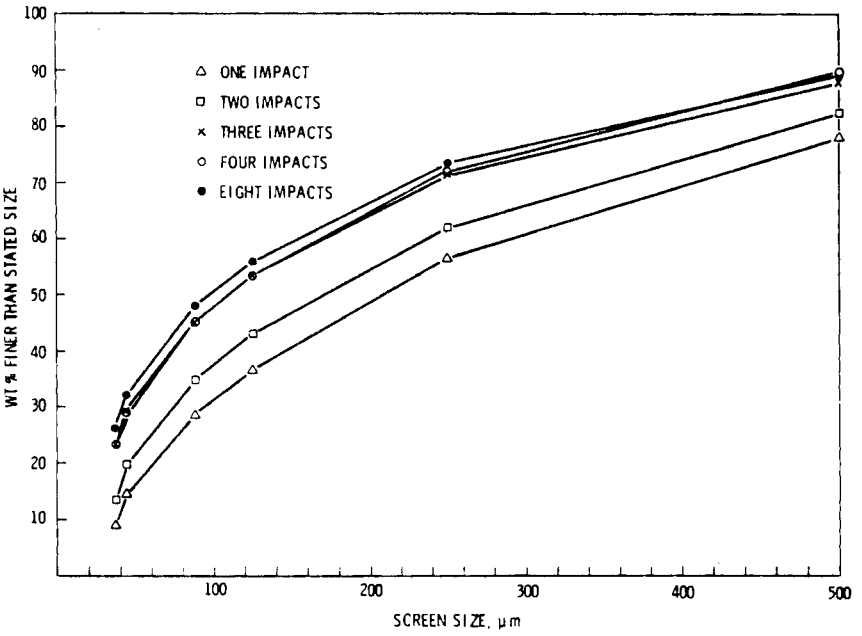

Figure 4. Sieve analysis results of multiple-impact testing.

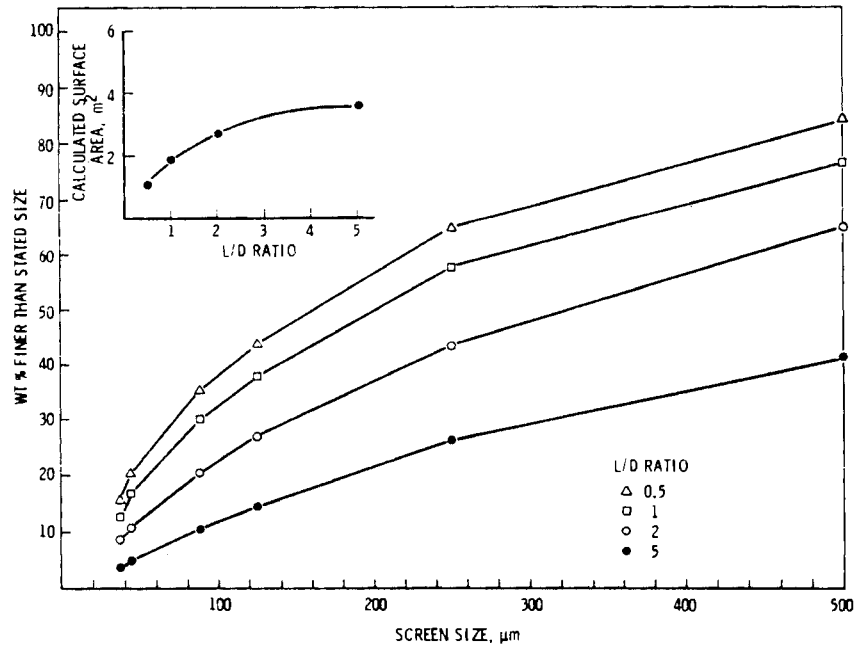

Figure 5. Sieve analysis results on soda-lime-silica glass of various L/D ratios. The inset shows (calculated) surface area as a function of L/D ratio.

A.3.4 Energy Equivalence Experiment.

Since impact energy was used as a variable in much of this work, an experiment was done to demonstrate that, at least within a reasonable range, equivalent impact damage could be produced by various combinations of mass and drop height. To do the experiment, an energy of 113J (83.2 ft-lb) was produced by four combinations of mass and height. The sieving results are shown in Figure 6. It is seen that differences in particle sizing are small and show no systematic trend with mass and height. The difference in hammer velocity was not large in this case, only varying from 3.71 to 4.88 m/s. Larger differences in hammer velocity might produce somewhat different results, but the velocity used in our tests is within a factor of 10 of drop accidents (13.4 m/sec is attained in a 9.1 m free fall) and shipping accidents [25 m/sec for a 90 km/h (60 mph) truck]. Since the driving force for impact damage is a shock wave traveling at a sonic velocity in the solid, an order of magnitude variations in hammer velocity should not be a prime factor influencing glass fracturing.

A.3.5 Effect of Devitrification on Impact Properties

Properly performed, devitrification can strengthen glasses. For example, the tensile strength of devitrified Corning glass 9617 is roughly three times that of the same glass in the vitreous state. In the best case, devitrification results in a body approaching a fine-grained polycrystalline ceramic, with very little glassy phase remaining. Devitrified waste glass is also tougher under some conditions, as has been found by German workers.[3] To evaluate the influence of devitrification, two glasses were impacted in both the vitreous and devitrified states.

The first glass examined was Corning Type 9617, a typical glass-ceramic. Specimens of this glass were tested in both the vitreous form and after devitrification according to a typical schedule (800^{o}C-31 min nucleation + 1150^{o}C-60 min growth). The material is >90% crystalline after this treatment. Figure 7 shows a comparison of these two conditions with a standard soda-lime-silica glass at several energies ranging from 27 to 217J (20-160 ft-lb). The devitrified product is marginally better than the

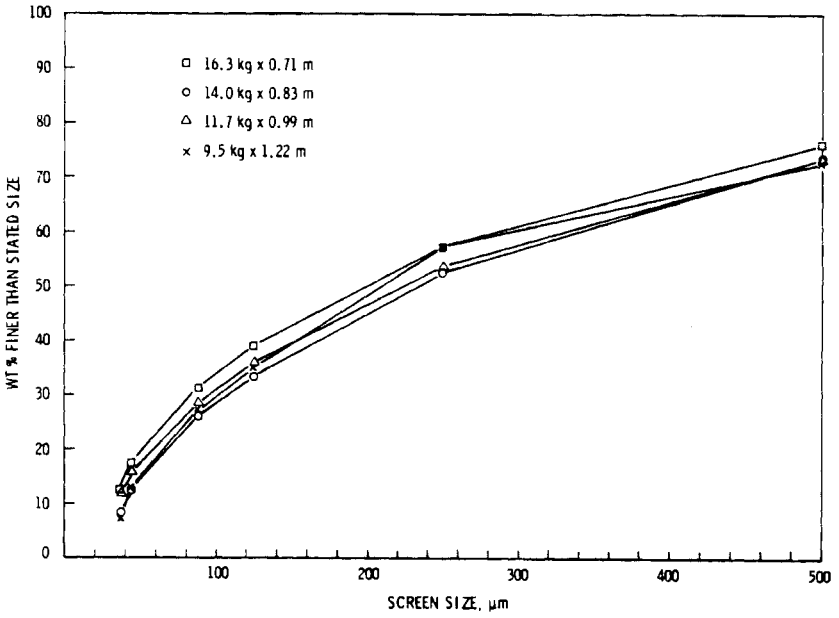

Figure 6. Sieve analysis results of equivalent energy delivered at different hammer velocity.

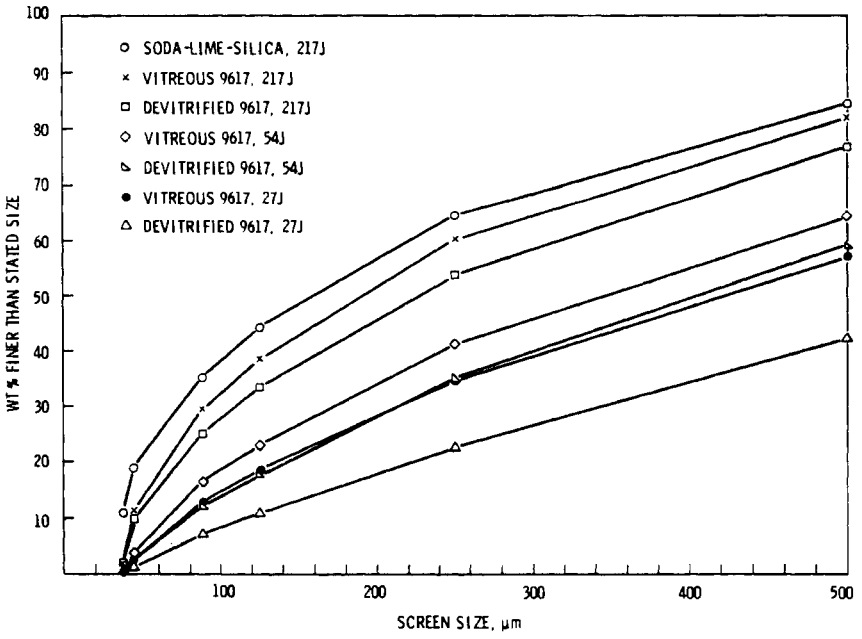

Figure 7. Sieve analysis results for vitreous and devitrified Corning 9617 glass at several impact energies.

vitreous at high energies and improves with decreasing energy. It is noteworthy that results from both of the sample conditions of 9617 glass are markedly superior to soda-lime-silica glass in terms of the amount of -37 μm fines, and are in fact the best observed in any of our glass impact work. This difference is apparently a result of composition. Since the Type 9617 specimens were only 0.64 cm thick, two pieces were used in each test. The soda-lime-silica was also tested in an identical configuration so that results would be comparable.

Comparison of vitreous versus partially devitrified simulated waste glass was made using composition 77-260, the AGNS glass. The vitreous specimens were prepared by melting at 1100°C, then cooling 2 h in a 600°C furnace which was then shut off. Devitrified specimens were prepared by cooling from 1100°C at 6.25 °C/h. This treatment resulted in about 30 vol% crystals, mainly $Gd_2Ti_2O_7$ and a rare earth apatite, $Ca_3(RE)_7(SiO_4)_5(PO_4)O_2$. Figure 8 shows sieving results after impact at 217J and shows no noteworthy differences between the two specimen conditions in regard to impact performance.

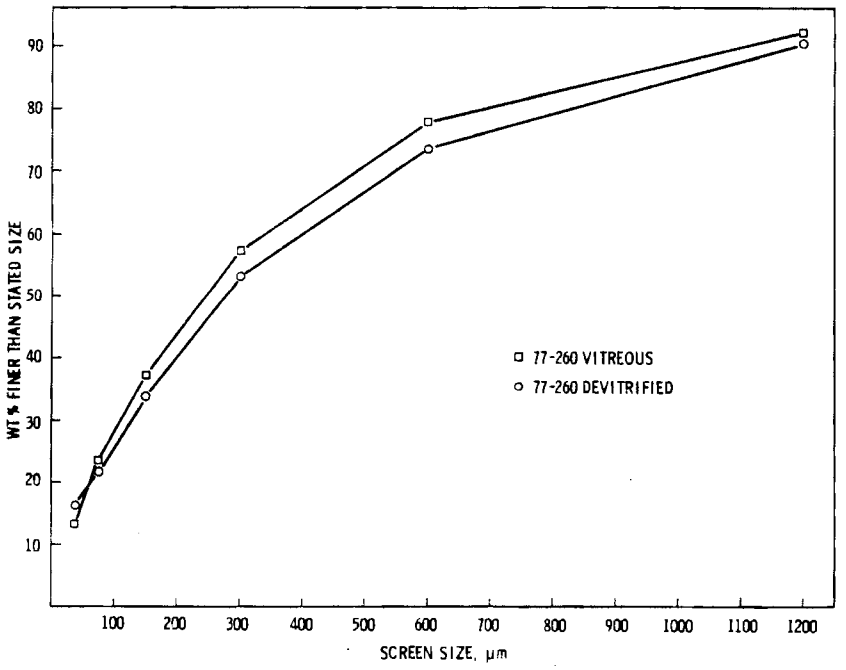

Figure 8. Sieve analysis results for Type 77-260 glass in the vitreous and devitrified state.

The difference between these results and those of the German workers is probably explainable in terms of the impact severity. Their impact was ∿60J and the specimen was substantially larger, about six times the volume of ours. The impact test used in our work is more severe because the relevant impacts are much greater than 60J. Earlier severe impact tests involving glass-filled canisters conducted at Pacific Northwest Laboratory,[1] involving energies to ∿8200J found no detectable difference between vitreous and devitrified simulated waste glasses. These glasses were not specifically designed or processed for devitrification as the German glasses were.

A.3.6 Surface Area as a Function of Impact Energy

During the impact event, some of the energy provided by the falling mass is used to create new surface area in the fracturing glass. For purposes of prediction, it would be convenient if there were a simple relationship between the amount of surface area created in a sample and the amount of energy involved in the impact. In order to see whether such a relationship existed, even for our lab-scale tests, two glasses, soda-lime-silica plate glass and ICM-11, were impacted over a fairly wide range of energies, 27 to 1900J. The surface areas of the resulting glass were determined by the B.E.T. technique. Results are plotted in Figure 9. Note that the impact damage in soda-lime-silica is apparently described by a simple function, while that in ICM-11 glass appears to show a saturation of damage. The saturation may be because of the abundance of undissolved rare earth oxides present in this glass.

For both of these glasses, then, surface area is a fairly simple function of impact energy over the range of energies covered by lab-scale tests. The predictive capacity for large canisters is at present non-existent because of the difficulty of determining the fraction of the impact which actually would be used to crush glass, deform canister metal, rebound, etc. The present utility of the surface area versus energy correlation will be to compare different glasses.

It is also instructive to assess the fraction of the impact energy which actually was utilized in creating new surface area. The fracture surface energy of soda-lime-silica glass at room temperature is reported to be

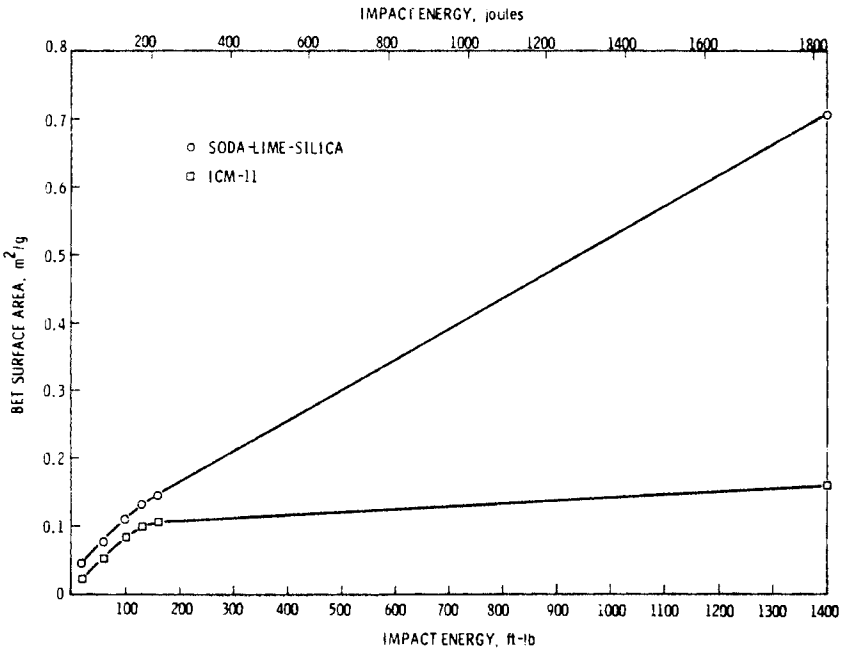

Figure 9. B.E.T. surface area as a function of impact energy for soda-lime-silica and ICM-11 glass.

3.85 J/m^2.(4) Based on the slope of the soda-lime-silica line in Figure 9, a surface energy of 1.1 x 10^{-3} m^2/J is calculated, indicating that only about 0.5% of the impact energy is used to create new surface area. The rest is apparently dissipated in other forms. Figure 10 shows results for glass ICM-11 and soda-lime-silica glass which were impacted at 217J, and simulated Hanford waste glass which was sampled from the most heavily damaged area of canister KT-14, weighing 2000 kg and dropped 7.6 m (Energy = 1.5 x 10^5J).

A.3.7 Fine Particle Sizes Produced by Impact

Glass particles with a diameter less than ca. 10 μm represent a respiration hazard.(5) Sedimentation size analysis was used to evaluate the fraction present at this diameter. Figure 10 shows three curves representing three glasses under two impact conditions. ICM-11 [PW-4-b(2.0)73-1] and soda-lime-silica glasses were impacted at 217 J, while simulated Hanford

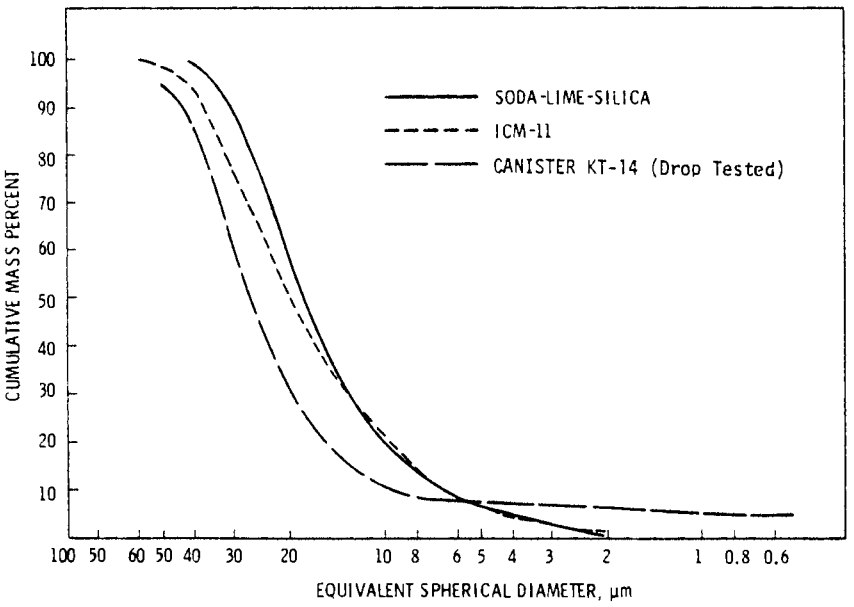

Figure 10. Subsieve size analysis for two glasses impacted in the lab test, as well as glass sampled from an actual drop test.

waste glass was sampled (~5 wt%) from the most heavily damaged area of canister KT-14, weighing 2000 kg and dropped 7.6 m. The -10 μm fraction of the first two is fairly small at (20% @ -44 μm x 14% @ -10 μm) = 2.8% for soda-lime-silica glass. For ICM-11 glass, the fraction is 2.4%. The respirable portion of the glass from canister KT-14 is even smaller at 0.13%. Apparently, these single-impact processes, even at high energies, are not very effective in producing fine particles.

A.3.8 Glass Ranking

Figure 11 is a compilation of sieving data on a variety of glasses, all impacted at an energy of 217J and all of the same size and shape. Table 1 is a brief description of all the glasses. From the data, the following observations can be made:

(1) Fused SiO_2 is the worst performer.

(2) Both 76-101 and 73-1 frits are superior in impact performance to the corresponding candidate waste glasses, 76-68 and 72-68 respectively.

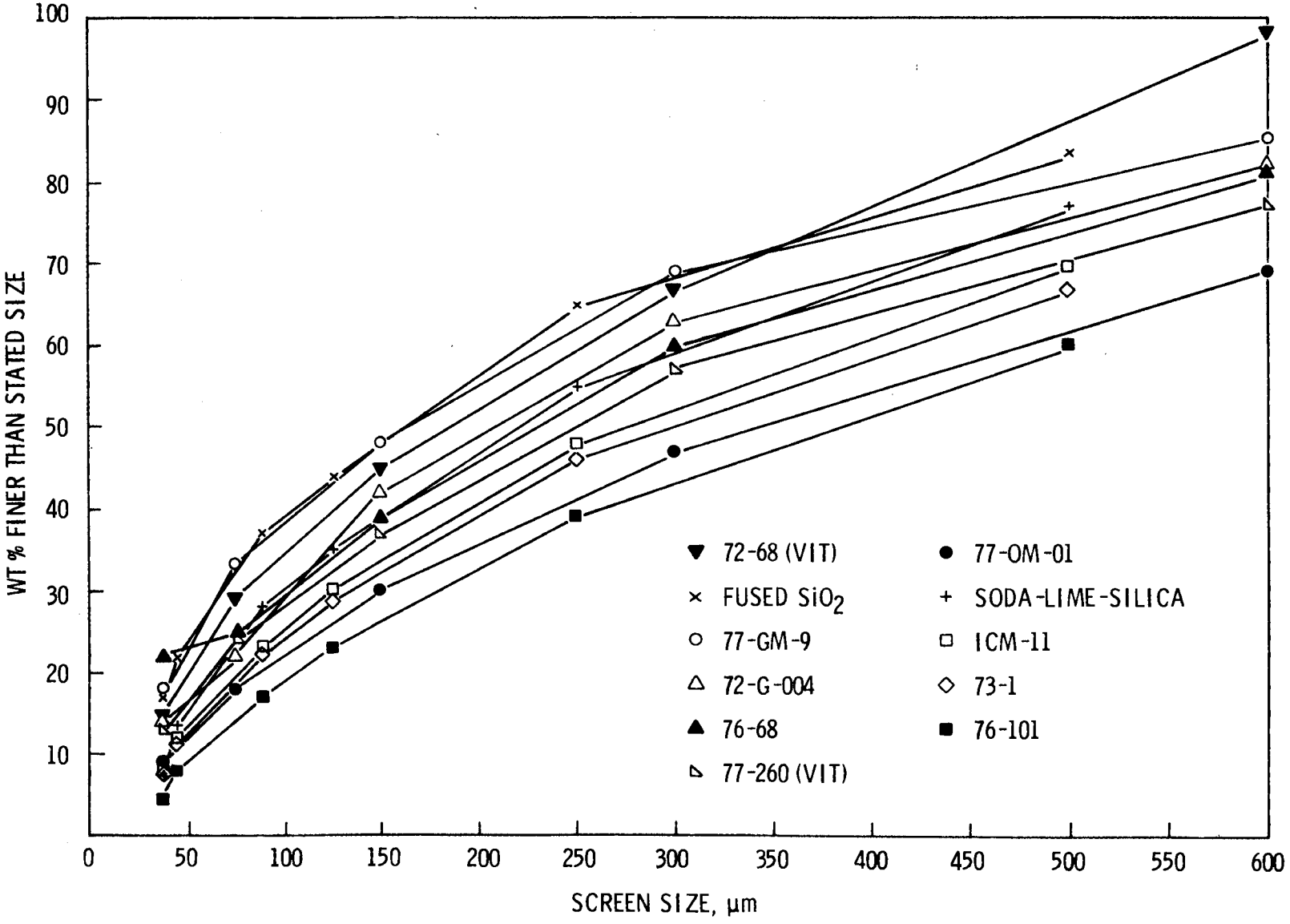

Figure 11. Plot of sieving data on a fairly wide variety of glasses.

(3) Most waste glass compositions are similar in impact behavior.

(4) Soda-lime-silica glass is similar to many of the candidate waste glasses as regards impact behavior judged from sieving.

(5) The shape of the curves is very similar, the main difference being in the amount of fine particles generated.

It is quite common in glass science to correlate test results with factors such as the percentage of silica or the oxygen/silicon ratio. Good correlations have been made in the past with fundamental properties like density and elastic moduli.[6] An attempt was made to make such a correlation for the impact data. The weight percentage of fines less than 37 μm in diameter was used as a rough performance index, and was plotted as a function of either silica content or O/Si ratio. These are plotted in Figures 12 and 13; it is clear that no simple correlation with O/Si ratio exists. The scatter implicit in the test (±5%) increases the difficulty of establishing clearcut correlations.

The line in Figure 12 indicates that some rough correlation <u>might</u> exist between silica content and fines generated. In the impact machine used for this work, abundant energy is available for specimen fracture. At the instant of failure, the specimen contains strain energy amounting to $K\sigma_f^2/2E$ where K = a constant, σ_f = fracture stress and E is Young's modulus. This energy is then converted to new surface area after the specimen fracture, which means that the higher the strain energy, the more fines will be produced. The shape of the line in Figure 12 would indicate that either the fracture strength goes through a minimum with silica content, or Young's modulus goes through a maximum. In the absense of any data on these properties for most of these glasses, the "relationship" is best regarded as fortuitous.

A word is in order regarding the general shape of the sieving curves in this report. Within the limits of the original sample size, the single impact of a brittle solid is regarded as a process which would ideally produce a classic bell-shaped distribution of particle sizes. Figure 14 shows three curves for typical glasses, and also includes a curve representing a cumulative Gaussian distribution. It is seen that there is not very much similarity in shape. When compared with the particle sizing occurring in other

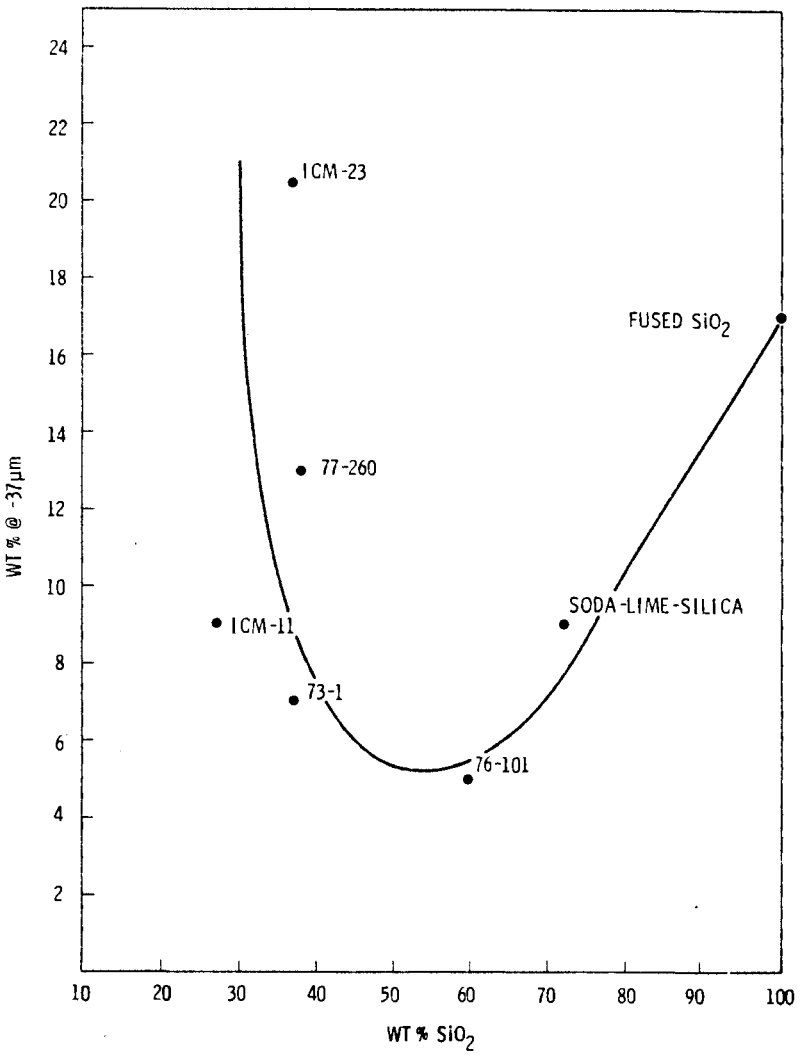

Figure 12. Attempted correlation of Impact damage as a function of silica content.

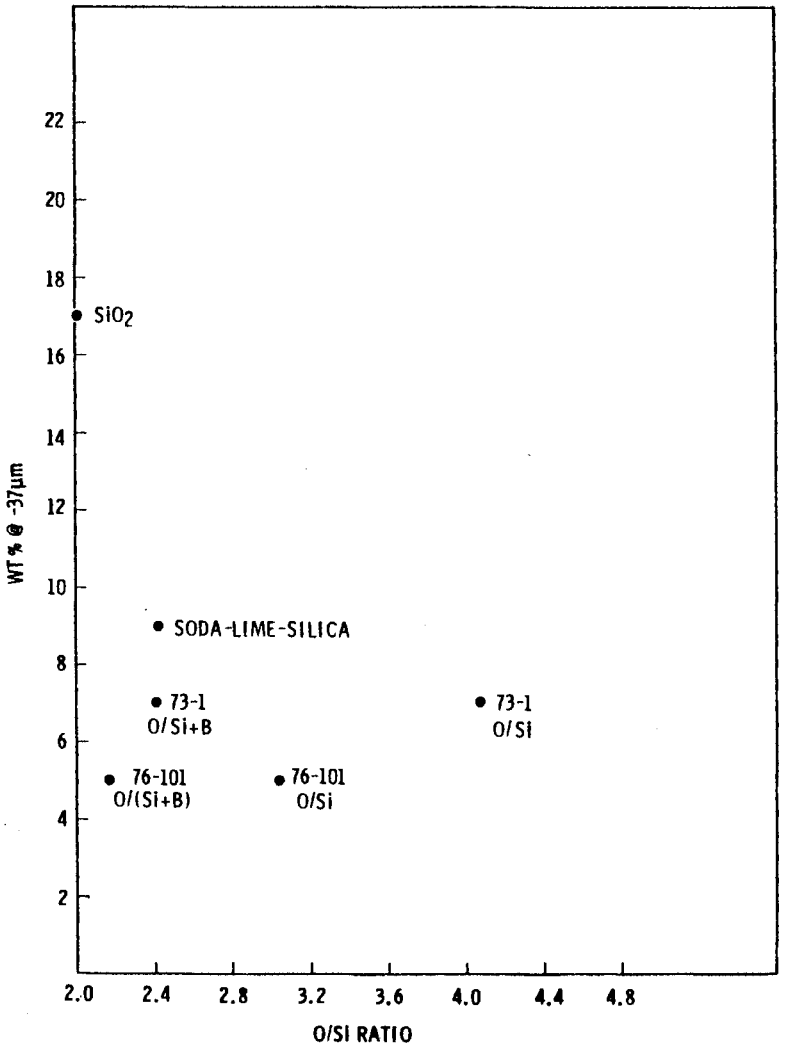

Figure 13. Same as Figure 12, except as a function of O/Si ratio.

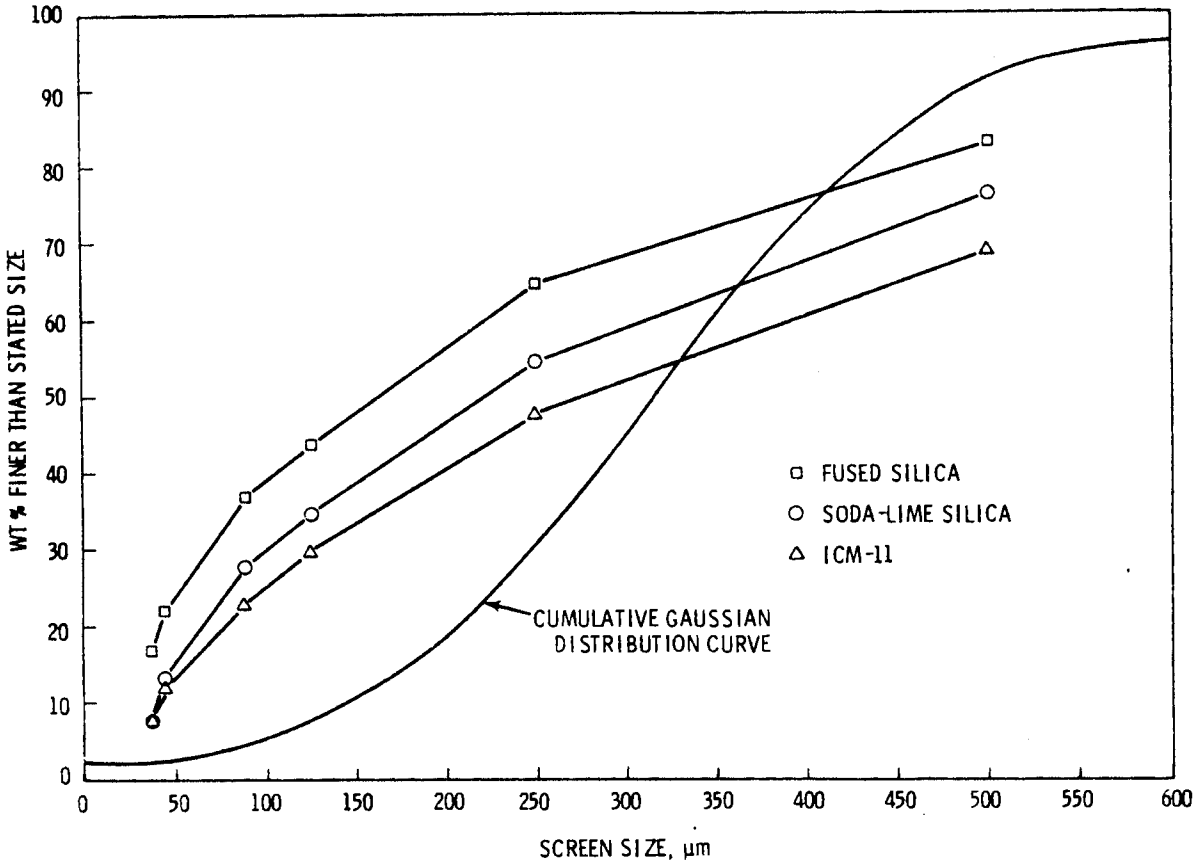

Figure 14. Sieve sizing data for three typical glasses, compared to Gaussian distribution.

size reduction processes such as ball mills, jaw crushers, and hammer mills,[7] the present data is closer to a Gaussian distribution than the output of any of these devices, which involve either multiple impacts and/or a mechanism for entrapping a particle and impacting it until it can pass through a gated opening. The single impact process does not involve this process of selection, but multiple impacts are probably present as the weight comes to rest. Also, the Gaussian curve is asymptotic at its end points, whereas all of our data must necessarily intersect the (0,0) point. This intersection was not drawn in the curves shown here because the route taken to reach zero was unknown.

B. TENSILE STRENGTH

B.1 INTRODUCTION

While the strength of the glass plays a role in the impact process, an impact serious enough for concern will fracture the glass; the concern in Section A above is mainly one of extent and resultant particle size. In addition, the strength of the glass per se is relevant for long-term storage because of several factors:

1. Because the canisters are large, the glass will contain residual thermal stress in addition to those which will have caused cracking near the canister wall during fabrication. These stresses will also change as the amount of heat generated by radioactive decay decreases.

2. In the presence of water or water vapor, it is a well-known fact[8] that glass exhibits static fatigue; that is, the stress to cause failure decreases with time.

3. Radiation-induced or devitrification-induced volume changes will produce additional stresses.

Consideration of the above points signals the need for at least some data on the strength of the waste glass. The objective of the work done on strength was to adapt a testing method such that it would be used even on highly radioactive glass with relative ease so these data could be collected.

B.2 EXPERIMENTAL METHOD

The "Strength" of a glass article is a rather nebulous quantity, and is a function of both the surface condition (strength-limiting flaws) and the testing method (volume of material under stress and knowledge of stress at failure site). The ceramic literature contains many good reviews of this subject; one of them is contained in Chapter 13 of Reference 6. The objective of this work was to define a strength test yielding useful numbers for design and capable of at least detecting large deviations from baseline measurements which would result from such factors as devitrification, etc.

The requirements of the strength test were that it would:

1. Require only a simple specimen geometry, one easy to obtain in a hot cell if desired.
2. Be self-aligning in a test fixture, so that only a minimum of critical handling would be involved and so that parasitic stresses would be eliminated. Parasitic stresses such as unknown bending moments can produce very misleading data in brittle materials.
3. Be an accepted method with at least some background in brittle materials.

In view of the above requirements, the test which emerged as the most feasible was the so-called Brazilian or splitting tensile test. It is used quite extensively for concrete (ASTM 946-64T) and has been used by other workers[9] in the nuclear waste area for evaluating crystalline forms. The diagram of Figure 15 shows the test configuration. The specimen can be prepared simply by diamond-sawing to parallelism a core-drilled sample. It will roll for alignment between the parallel pressure plates of the test machine. The pads shown are a critical part of the test; they are used to prevent high point loading at the glass-platen contacts, which would cause crushing and premature failure. A number of materials were tried as pads, including aluminum, IBM cards, Teflon*, brass and several types of single-ply

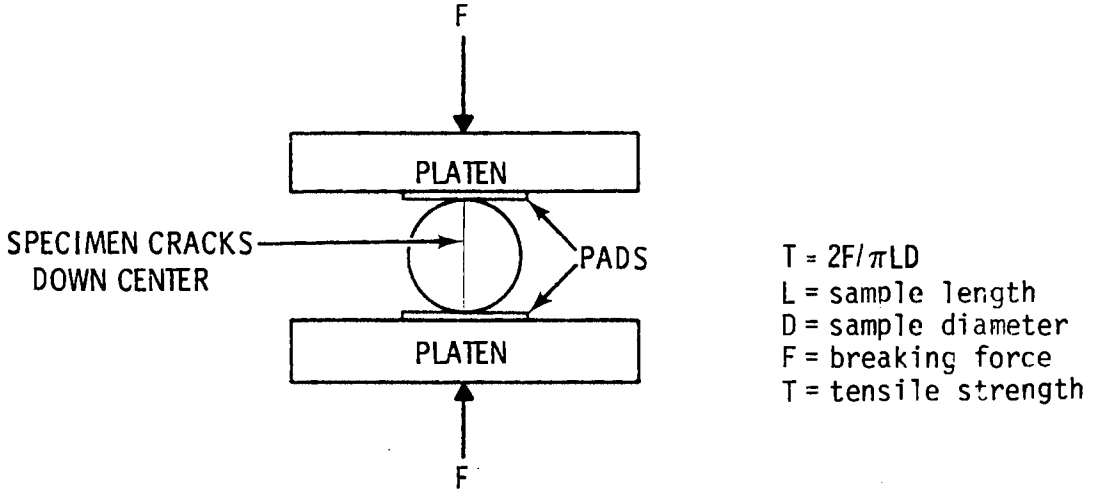

Figure 15. Diagram of experimental arrangement used in Brazilian splitting tensile test.

*duPont, Wilmington, DE.

and multiple-ply wood. Balsa wood, with its grain oriented perpendicular to the line contact formed between cylinder and plate, was finally selected as the best pad material.

B.3 RESULTS AND DISCUSSION

The splitting tensile test was used on a group of soda-lime-silica glass rods as well as some core-drilled specimens of ICM-11 glass. An Instron* testing machine was used; the loading speed was 0.05 cm/min. The results are shown in Table 2. The standard deviations, while large, are not excessively so for glass testing. As a consequence, primarily of the large scatter, there is little if any difference between the measured strengths on a statistical basis (no difference at the 90% level). The ICM-11 appears to be somewhat weaker, which would be expected from its rather large population of strength-limiting flaws produced by undissolved rare earth oxides. Though the strength is marginally higher for the soda-lime-silica glass, the standard deviation is also higher. The splitting test is recommended as an evaluation of tensile strength of simulated and actual waste-containing glasses, as well as other homogeneous waste forms such as sintered supercalcine or devitrified glass-ceramic.

TABLE 2. Splitting Tensile Test Results

Type of Glass	Number of Samples	Average Strength mPa (psi)	Standard Deviation mPa (psi)
Soda-Lime-Silica	32	47.67 (6913)	12.55 (1820)
ICM-11	29	37.18 (5393)	7.01 (1017)

*Instron Corp., Canton, MA.

A.4 CONCLUSIONS

1. Compositional changes within the ranges expected for waste-containing glasses are not likely to have a large effect on impact performance.
2. In the range of energies tested, devitrification has little effect on impact performance.
3. The impact test is sufficiently specimen geometry dependent to justify caution when changing configurations used in lab-scale tests.
4. In the range of energies tested, surface area of generated particles was a simple function of impact energy for soda-lime-silica and a simulated waste-containing glass.

B.4 CONCLUSIONS

The Brazilian or splitting tensile test is applicable for strength determination on waste glasses and meets the requirements for such a test.

ACKNOWLEDGMENT

This work was performed for the U.S. Department of Energy under Contract EY-76-C-06-1830. The technical assistance of S. D. Tomich and R. A. Wheeler in the conduct of this work is gratefully acknowledged.

REFERENCES

1. T. H. Smith and W. A. Ross, Impact Testing of Vitreous Simulated High-Level Waste in Canisters, BNWL-1903, Pacific Northwest Laboratory, (May, 1975).

2. R. M. Wallace and J. A. Kelley, An Impact Test for Solid Waste Forms, DP-1400 Savannah River Laboratories (March 1976).

3. A. K. De, B. Luckscheiter, W. Lutze, G. Malow, and E. Schiewer, "Development of Glass Ceramics for the Incorporation of Fission Products," Amer. Cer. Soc. Bull. 55(5) (1976).

4. S. M. Wiederhorn, "Fracture Surface Energy of Glass, Journal Amer. Cer. Soc. 52(2) 99 (1969).

5. T. T. Mercer, Aerosol Technology in Hazard Evaluation, Academic Press (1973).

6. G. W. Morey, The Properties of Glass, Second Edition, Reinhold Publishing Corp., pp 305, 272,224 (1954).

7. C. G. Lowrison, Crushing and Grinding, The Size Reduction of Solid Materials, CRC Press, p 71 (1974).

8. E. Orowan, "The Fatigue of Glass Under Stress," Nature, 154, 341 (September 9, 1944).

9 R. H. Marion and J. K. Johnstone, Parametric Study of the Diametral Compression Tests for Ceramics, SAND-75-0347, Sandia Laboratories (July 1975).

APPENDIX A

Compositions of Glasses Tested

APPENDIX A. APPROXIMATE COMPOSITION[a] OF GLASSES TESTED

	Fused SiO_2	Soda-Lime-Silica	73-1 Frit	76-101 Frit	77-260	ICM-11	Hanford Waste Glass	72-68[c]	Typical Rhyolite[f]
SiO_2	100	72	37	59.7	36.0	24.7	46.6	27.8	73.3
B_2O_3			15.1	14.2	9.0	10.1	13.2	11.3	
Na_2O		15	5.5	11.2	11.1	3.7	13.7	4.1	3.6
TiO_2					6.0		3.0		
Li_2O							3.0		
K_2O			5.5		2.0	4.3		5.0	4.2
CaO		9	2.0	3.0	1.0	1.3	0.6	1.5	1.8
ZnO			28.9	7.5		19.3		21.7	
Fe_2O_3					1.2	2.8	3.6	1.1	1.7
Al_2O_3		1			2.0		7.0		13.6
MnO_2					0.1		0.6		0.5
NiO							0.7		
Cr_2O_3						0.2	0.4	0.3	
SrO			2.0		0.3	2.0	2.2	2.3	
TiO_2				4.5			0.2		
Bi_2O_5							1.0		
P_2O_5					2.4	1.6	1.7	0.5	0.2
CeO_2					0.9		1.0		
ZrO_2					1.5	2.9	1.0	3.7	
MoO_3					2.0	3.7		4.8	
RE_2O_3					12.6				
MgO		3	2.0			1.3		1.5	0.6
BaO			2.0		0.6	2.2		2.7	
CuO					3.0				
Rb_2O					0.1				
Y_2O_3					0.2				
RuO_2					0.9				
Rh_2O_3					0.2				
PdO					0.5			0.1	
Ag_2O						0.1		0.1	
CdO					0.2	0.4		0.6	
TeO_2						0.6		0.1	
NiO						0.2		0.2	
Co_3O_4						12.5		6.1	
Rare Earth Oxides[d]						6.2		4.6	
Didymium Oxides[e]									
U_3O_8					5.3				
Cs_2O					0.8				
La_2O_3					0.5				

[a] As wt% oxide

[b] Composition of this glass is proprietary.

[c] There are several glasses bearing the designation 72-68. They are from similar glass of known composition. The one noted contains no UO_2, and is made from 73-1 frit and PW-4b-2 calcine, 3:1 by wt.

[d] Commercial rare earth mix nominal oxide composition: 0.2% Y_2O_3, 24% La_2O_3, 48% CeO_2, 5% Pr_6O_{11}, 17% Nd_2O_3, 3% Sm_2O_3, 2% Gd_2O_3, and 0.8% other rare earth oxides.

[e] Commercial didymium nominal oxide composition: 4% Y_2O_3, 37% La_2O_3, 2% CeO_2, 10% Pr_6O_{11}, 36% Nd_2O_3, 5% Sm_2O_3, 4% Gd_2O_3 2% Dy_2O_3, 0.2% Ho_2O_3, 0.4% Er_2O_3, and <0.1% of each other rare earth oxides.

[f] Chemical composition of the three natural glasses was not available in the literature, so these glasses are represented by an average of three rhyolites which did not differ markedly in composition.

DISTRIBUTION

No. of Copies

UNITED STATES

A. A. Churm
DOE Chicago Patent Division
9800 South Cass Avenue
Argonne, IL 60439

R. E. Cunningham
Deputy Director for Fuels and Materials
Nuclear Regulatory Commission
Silver Springs, MD 20910

Assistant Director for Radioactive Waste Management Branch
NRC Division of Materials and Fuel Cycle Facility Licensing
Washington, DC 20545

D. M. Rohrer
United States Nuclear Regulatory Commission
Washington, DC 20555

John Martin
United States Nuclear Regulatory Commission
Washington, DC 20555

W. G. Belter
DOE Division of Biomedical and Environmental Research
Earth Sciences Branch
Washington, DC 20545

W. A. Brobst
DOE Division of Environmental Control Technology
Washington, DC 20545

No. of Copies

W. E. Mott
DOE Division of Environmental Control Technology
Washington, DC 20545

R. B. Chitwood
DOE Division of Nuclear Power Development
Washington, DC 20545

T. C. Chee
DOE Office of Nuclear Waste Management
Washington, DC 20545

C. R. Cooley
DOE Office of Nuclear Waste Management
Washington, DC 20545

Sheldon Meyers
DOE Office of Nuclear Waste Management
Washington, DC 20545

R. G. Romatowski
DOE Office of Nuclear Waste Management
Washington, DC 20545

C. A. Heath
DOE Office of Nuclear Waste Management
Washington, DC 20545

G. Oertel
DOE Office of Nuclear Waste Management
Washington, DC 20545

No. of Copies

A. F. Perge
DOE Office of Nuclear Waste Management
Washington, DC 20545

D. L. Vieth
DOE Office of Nuclear Waste Management
Washington, DC 20545

R. D. Walton
DOE Office of Nuclear Waste Management
Washington, DC 20545

J. Neff, Program Manager
Department of Energy
Columbus Program Office
505 King Avenue
Columbus, OH 43201

J. B. Whitsett
DOE Idaho Operations Office
P.O. Box 2108
Idaho Falls, ID 83401

John Van Cleve
DOE Oak Ridge Operations Office
P.O. Box X
Oak Ridge, TN 37830

E. S. Goldberg
DOE Savannah River Operations Office
P.O. Box A
Aiken, SC 29801

27 DOE Technical Information Center

A. P. Roeh, Manager
Allied Chemical Corporation
550 2nd Street
Idaho Falls, ID 83401

No. of Copies

J. R. Berreth
Allied Chemical Corporation
550 2nd Street
Idaho Falls, ID 83401

R. A. Brown
Allied Chemical Corporation
550 2nd Street
Idaho Falls, ID 83401

C. A. Hawley
Allied Chemical Corporation
550 2nd Street
Idaho Falls, ID 83401

D. A. Knecht
Allied Chemical Corporation
550 2nd Street
Idaho Falls, ID 83401

Allied Chemical Corporation
(File Copy)
550 2nd Street
Idaho Falls, ID 83401

M. D. McCormack
E.G. & G.Idaho, Inc.
P.O. Box 1625
Idaho Falls, ID 83401

W. C. Seymour
E.G. & G. Idaho, Inc.
P.O. Box 1625
Idaho Falls, ID 83401

R. A. Buckham
Allied-General Nuclear Service
P.O. Box 847
Barnwell, SC 29812

A. Williams
Allied-General Nuclear Service
P.O. Box 847
Barnwell, SC 29812

No. of
Copies

Keith Flynn
Argonne National Laboratory
9700 South Cass Avenue
Argonne, IL 60439

J. L. Jardine
Argonne National Laboratory
9700 South Cass Avenue
Argonne, IL 60439

M. M. Steindler/L. E. Trevorrow
Argonne National Laboratory
9700 South Cass Avenue
Argonne, IL 60439

J. M. Batch
Battelle Memorial Institute
505 King Ave.
Columbus, OH 43201

Wayne Carbiener
Battelle Memorial Institute
505 King Ave.
Columbus, OH 43201

J. D. Duguid
Battelle Memorial Institute
505 King Ave.
Columbus, OH 43201

R. E. Heineman
Battelle Memorial Institute
505 King Ave.
Columbus, OH 43201

Battelle Memorial Institute
Office of Nuclear Waste
Isolation
Attn: Beverly Rawles
505 King Avenue
Columbus, OH 43201

No. of
Copies

J. Kircher
Office of Nuclear Waste
Isolation
Battelle Memorial Institute
505 King Ave.
Columbus, OH 43201

Don Moak
Battelle Memorial Institute
505 King Ave.
Columbus, OH 43201

Ken Yates
Battelle Memorial Institute
505 King Ave.
Columbus, OH 43201

Brookhaven National Laboratory
Reference Section
Information Division
Upton, NY 11973

Paul W. Levy
Brookhaven National Laboratory
Upton, NY 11973

M. Steinberg
Brookhaven National Laboratory
Upton, NY 11973

Combustion Division
Combustion Engineering, Inc.
Windsor, CT 06095

B. Adams
Corning Glass Works
Technical Staffs Division
Corning, NY 14830

E. Vejvoda, Director
Chemical Operations
Rockwell International
Rocky Flats Plant
P.O. Box 464
Golden, CO 80401

No. of
Copies

J. L. Crandall
E. I. duPont DeNemours and Company
Savannah River Laboratory
Aiken, SC 29801

H. L. Hull
E. I. duPont DeNemours and Company
Savannah River Laboratory
Aiken, SC 29801

R. G. Garvin
E. I. duPont DeNemours and Company
Savannah River Laboratory
Aiken, SC 29801

D. L. McIntosh
E. I. duPont DeNemours and Company
Savannah River Laboratory
Aiken, SC 29801

J. A. Kelley
E. I. duPont DeNemours and Company
Savannah River Laboratory
Aiken, SC 29801

S. D. Harris, Jr.
E. I. duPont DeNemours and Company
Savannah River Laboratory
Aiken, SC 29801

Robert Maher
E. I. duPont DeNemours and Company
Savannah River Laboratory
Aiken, SC 29801

No. of
Copies

S. Mirschak
E. I. duPont DeNemours and Company
Savannah River Laboratory
Aiken, SC 29801

J. K. Okeson
E. I. duPont DeNemours and Company
Savannah River Laboratory
Aiken, SC 29801

M. S. Plodinec
E. I. duPont DeNemours and Company
Savannah River Laboratory
Aiken, SC 29801

A. S. Jennings
E. I. duPont DeNemours and Company
Savannah River Laboratory
Aiken, SC 29801

Leon Meyers
E. I. duPont DeNemours and Company
Savannah River Laboratory
Aiken, SC 29801

H. Henning
Electric Power Research Institute
3412 Hillview Avenue
P.O. Box 10412
Palo Alto, CA 94301

Environmental Protection Agency
Technology Assessment Division (AW-559)
Office of Radiation Programs
Washington, DC 20460

No. of Copies

R. G. Barnes
General Electric Company
175 Curtner Avenue (M/C 858)
San Jose, CA 95125

L. H. Brooks
Gulf Energy and Environmental Systems
P.O. Box 81608
San Diego, CA 92138

D. C. Fulmer
Savannah River Operations Office
P.O. Box A
Aiken, SC 29801

3 Los Alamos Scientific Laboratory (DOE)
P.O. Box 1663
Los Alamos, NM 87544

C. J. Kershner
Monsanto Research Corporation
Mound Laboratory
P.O. Box 32
Miamisburg, OH 45342

John Pomeroy
Technical Secretary
National Academy of Sciences
Committee of Radioactive Waste Management
National Research Council
2101 Constitution Avenue
Washington, DC 20418

Stewart Farber
New England Power Company
280 Melrose Street
Providence, Rhode Island 02901

No. of Copies

2 J. P Duckworth
Plant Manager
Nuclear Fuel Services, Inc.
P.O. Box 124
West Valley, NY 14171

J. G. Cline, General Manager
NYS Energy Research and Development Authority
230 Park Avenue, Rm 2425
New York, NY 10017

2 Oak Ridge National Laboratory (DOE)
Central Research Library
Document Reference Section
P.O. Box X
Oak Ridge, TN 37830

E. H. Kobish
Solid State Division
Oak Ridge National Laboratory
Oak Ridge, TN 37830

G. J. McCarthy
Pennsylvania State University
Materials Research Laboratory
University Park, PA 16802

Professor Guna Salvaduray
Materials Engineering
San Jose State University
San Jose, CA 95192

D. R. Anderson
Sandia Laboratories
Albuquerque, NM 87107

J. K. Johnstone
Sandia Laboratories
Albuquerque, NM 87107

No. of
Copies

W. Weart
Sandia Laboratories
Albuquerque, NM 87107

J. Sivinshi
Sandia Laboratories
Albuquerque, NM 87107

J. O. Blomeke
Union Carbide Corporation (ORNL)
Chemical Technology Division
P.O. Box Y
Oak Ridge, TN 37830

R. E. Blanco
Union Carbide Corporation (ORNL)
Chemical Technology Division
P.O. Box Y
Oak Ridge, TN 37830

E. Newman
Union Carbide Corporation (ORNL)
Chemical Technology Division
P.O. Box Y
Oak Ridge, TN 37830

A. L. Lotts
Union Carbide Corporation (ORNL)
Chemical Technology Division
P.O. Box Y
Oak Ridge, TN 37830

W. J. Lackey
Union Carbide Corporation (ORNL)
Chemical Technology Division
P.O. Box Y
Oak Ridge, TN 37830

T. Lindemer
Union Carbide Corporation (ORNL)
Chemical Technology Division
P.O. Box Y
Oak Ridge, TN 37830

No. of
Copies

D. E. Ferguson
Union Carbide Corporation (ORNL)
Chemical Technology Division
P.O. Box Y
Oak Ridge, TN 37830

H. W. Godbee
Union Carbide Corporation (ORNL)
Chemical Technology Division
P.O. Box Y
Oak Ridge, TN 37830

W. C. McClain
Union Carbide Corporation (ORNL)
Chemical Technology Division
P.O. Box Y
Oak Ridge, TN 37830

R. A. Beall
U. S. Department of Interior
Bureau
of Mines
Albany Research Center
1450 W. Queen Avenue
Albany, OR 97321

D. B. Stewart
U. S. Department of Interior
959 National Center
Geological Survey
Reston, Virginia 22092

R. G. Post
College of Engineering
University of Arizona
Tucson, AZ 85721

S. E. Logan
Los Alamos Technical
Associates, Inc.
P.O. Box 410
Los Alamos, NM 87544

No. of Copies

FOREIGN

2 International Atomic Energy Agency
Kartner Ring 11
P.O. Box 590
A-1011, Vienna, AUSTRIA

Rene Amavis
EURATOM
Health Physics Division
29, Rue Aldringer
Luxembourg, BELGIUM

G. G. Strathdee
Atomic Energy of Canada, Ltd.
W.N.R.E. Pinawa, Manitoba
ROE 1LO
CANADA

M. Tomlinson
Director of Chemistry and Materials Science Division
Atomic Energy of Canada Ltd.
Whiteshell Nuclear Research Establishment
Pinawa, Manitoba, CANADA

K. D. B. Johnson
Atomic Energy Research Establishment,
Harwell, Didcot,
Berks, ENGLAND

J. A. C. Marples
Atomic Energy Research Establishment
Harwell, Didcot,
Berks, ENGLAND

D. W. Clelland
United Kingdom Atomic Energy Authority
Risley, ENGLAND

No. of Copies

P. J. Regnaut
Centre d'Etudes Nucleaires de Fontenay-aux Roses
Boite Postale 6
92 - Fontenay-aux Roses
FRANCE

Dr. P. G. Alfredson
Chief, Chemical Technology Division
Australian Atomic Energy Commission
Research Establishment
Lucas Heights, New South Wales, 2232

Library
Studsvik Energiteknik AB
S-611 01Nykoping
SWEDEN

Bundesministerium fur Forschung und Technologie
Stressemannstrasse 2
5300 Bonn
WEST GERMANY

Center for Atomic Energy Documentation (ZAED)
Attn: Dr. Mrs. Bell
P. O. Box 3640
7500 Karlsruhe
WEST GERMANY

Hans W. Levi
Hahn-Meitner Institut
1 Berlin 39
Glienickerstr. 100
WEST GERMANY

No. of Copies

FOREIGN

E. R. Merz
Institut fur Chemische Technologie
Kernforschungsanloge Julich GmbH
D517 Julich
Postfach 365
Federal Republic
WEST GERMANY

R. Bonniaud
Center de Marcoule
B.P. 170
30200 Baguols-Sur-Ceze
FRANCE

C. Sombret
Centre de Marcoule
B.P. 170
30200 Baguols-Sur-Ceze
FRANCE

F. Laude
Centre de Marcoule
B.P. 170
30200 Baguols-Sur-Ceze
FRANCE

2 H. Krause
Kernforschungszentrum Karlsruhe GmbH (KfK)
Postfach 3640
D7500 Karlsruhe
WEST GERMANY

R. V. Amalraj
C.W.M.F. Project
P.O. Kalpakkam
Chingleput Dist.
Tamil Nadu, INDIA

No. of Copies

N. S. Sunder Rajan
Bhabha Atomic Research Centre
Goverment of India
Hall No. 5
Trombay
Bombay 8S
INDIA

Dr. Piero Risoluti,
AGIP NUCLEARE
c/o COMB Casaccia
C.P. 2400
Rome
ITALY

F. Gera
CHEN
CSN Casaccia L.I.S.
C.P. 2400, 00100
Rome
ITALY

S. Tashiro
Japan Atomic Energy Research Institute
Environmental Safety Research Laboratory
1-1-13, Shibashi
Minatopku, Tokyo
JAPAN

ONSITE

4 DOE Richland Operations Office

P. A. Craig
H. E. Ransom
M. W. Shupe
M. J. Zamorski

No. of Copies

ONSITE

11 Rockwell Hanford Operations

H. Badad
R. A. Deju
R. J. Gimera
J. D. Kaser
E. J. Kosiancic
M. J. Kupfer
C. M. Manry
J. H. Roecker
W. W. Schultz
D. D. Wodrich
File copy

3 Exxon Nuclear Company

S. J. Beard

Joint Center for Graduate Study

J. Cooper

2 United Nuclear Industries, Inc.

T. E. Dabrowski
A. E. Engler

Westinghouse Hanford Company

A. G. Blasewitz

78 Pacific Northwest Laboratory

S. M. Barnes
W. J. Bjorklund
H. T. Blair
W. F. Bonner
D. J. Bradley
A. Brandstetter

No. of Copies

R. A. Brouns
J. B. Brown, Jr.
J. L. Buelt
R. L. Bunnell (10)
H. C. Burkholder
L. A. Chick
T. D. Chikalla
M. O. Cloninger
R. D. Dierks
J. W. Finnigan
W. J. Gray
M. S. Hanson
J. C. Hartl
M. H. Henry (3)
O. F. Hill
L. K. Holton
J. H. Jarrett
Y. B. Katayama
W. S. Kelly
R. S. Kemper
D. E. Knowlton
D. K. Kreid
W. L. Kuhn
D. E. Larson
J. M. Lukacs
R. P. Marshall
S. A. McCullough
J. L. McElroy (3)
J. S. McPherson
G. B. Mellinger
J. E. Mendel
F. A. Miller
R. E. Nightingale
D. E. Olesen
C. R. Palmer
A. M. Platt
D. L. Prezbindowski (2)
F. P. Roberts
W. A. Ross
J. M. Rusin
D. H. Siemens
S. C. Slate
R. T. Treat
R. P. Turcotte (2)

No. of
Copies

ONSITE

H. H. Van Tuyl
J. W. Voss
J. W. Wald/W. E. Weber
J. H. Westsik, Jr.
L. D. Williams
W. K. Winegardner
Technical Information (5)
Publishing Coordination (2)